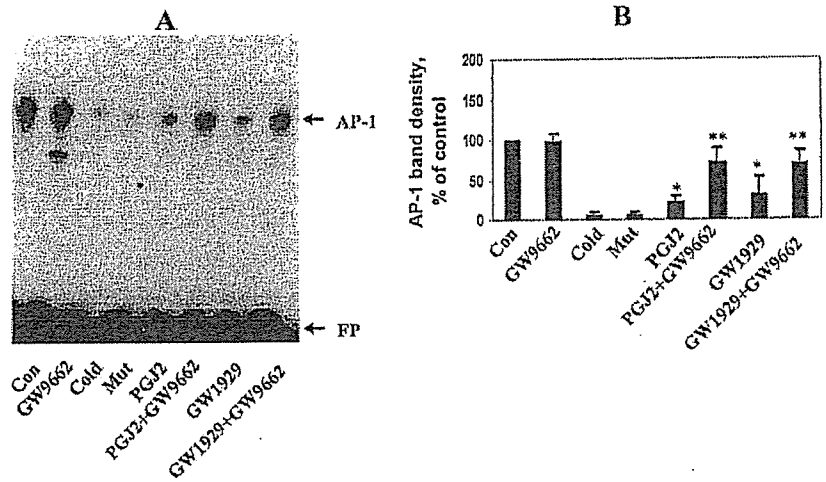

Fig. 6 AP-1 binding in cervical cancer cells is regulated through the PPARγ signaling pathway. CaSki cells were treated as indicated with vehicle control (*Con*), 20 μM 15d-PGJ2, 20 μM GW1929, 20 μM GW9662, or 20 μM GW9662 for 1 h before adding one of the above PPARγ activators for a total of 24 h. Nuclear extracts were prepared and subjected to EMSA using a CRE consensus radiolabeled probe (A). The CRE probe was mutagenized to show specificity of binding (*Mut*). A 100-fold molar excess of unlabeled AP-1 oligonucleotide was incubated with the radiolabeled probe/extract mixture for competition. *FP* indicates free probe. The bar graph (*B*) represents the mean of relative AP-1 binding as quantified by densitometry of at least three independent experiments for each treatment condition; *bars*, ±SD. * indicates significant difference as compared with the vehicle control. ** indicates significance of combination treatment as compared with PPARγ activators alone.

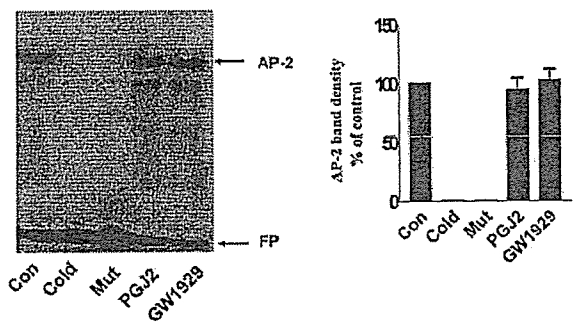

Fig. 7 AP-2 binding in cervical cancer cells is not regulated through the PPARγ signaling pathway. Nuclear extracts were prepared from CaSki cells treated for 24 h with the compounds as indicated: solvent control (*Con*), 20 μM 15d-PGJ2 or GW1929. Nuclear extracts were subjected to EMSA using an AP-2 consensus sequence radiolabeled probe, and protein-DNA complexes were visualized by autoradiography. The AP-2 probe was mutagenized to show specificity of binding (*Mut*). A 100-fold molar excess of unlabeled AP-2 oligonucleotide was incubated with the radiolabeled probe/extract mixture for competition (*Cold*). *FP* indicates free probe.

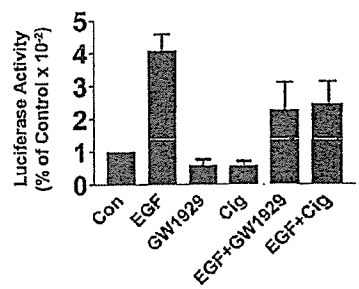

Fig. 8 Effects of PPARγ ligands and EGF on COX-2 promoter activity. CaSki cells were cotransfected with a human COX-2 promoter reporter construct (−327/+59) and an internal control plasmid as described in "Materials and Methods" and immediately treated as indicated with vehicle control (*Con*), 20 ng/ml EGF, 20 μM GW1929, 30 μM Cig, or 20 ng/ml EGF +20 μM GW1929 or +30 μM Cig for 24 h. After normalizing the results using the internal control plasmid, the vehicle control value was set as 100% activity. The bars represent the mean of at least four independent experiments for each treatment condition; *bars*, ±SD.

DISCUSSION

In this study, we demonstrated that COX-2 and PPARγ genes are expressed in both primary human cervical cancer tissues and the cervical cancer cell line CaSki. The expression of PPARγ in cells derived from the cervix has heretofore not been reported. Our results demonstrated reciprocal negative regulation between PPARγ and COX-2 gene expression, because up-regulation of COX-2 was coincident with down-regulation of PPARγ, and *vice versa*. The ability of PPARγ ligands to down-regulate COX-2 has also been reported in breast cancer cells and macrophages (31, 32), but was shown to up-regulate COX-2 expression in monocytes (38), synovial fibroblasts (39), and some colon cancer cells (17, 40). Taken together, these divergent results indicate that the qualitative nature of the interaction(s) between PPARγ and COX-2 (negative or positive) is tissue-specific and extrapolation of findings to different cell types cannot be made.

In light of our demonstration that PPARγ ligands negatively regulate COX-2 in cervical cancer cells, the strong expression of both PPARγ and COX-2 in primary cervical cancer

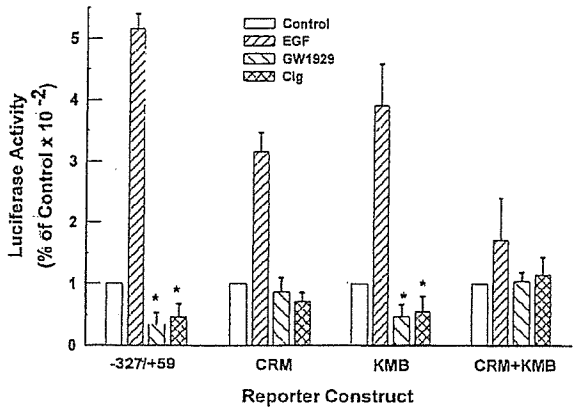

Fig. 9 Inhibition of COX-2 promoter activity by PPARγ ligands is mediated by the CRE binding site. CaSki cells were transfected with the −327/+59 COX-2 promoter construct or the mutant promoter constructs as indicated and immediately treated for 24 h with vehicle control (*Control*), 20 ng/ml EGF, 20 μM GW1929, or 30 μM Cig as designated in the figure key. After normalizing the results using an internal control plasmid as described in "Materials and Methods," the vehicle control value for each reporter construct was set as 100% activity. The *bars* represent the mean ± SD of at least four independent experiments for each condition. * indicates significant inhibition of activity as compared with vehicle controls. The CRM and CRM+KBM mutants showed no significant inhibition of activity after treatment of cells with the PPARγ activators.

is surprising and suggests aberrant interaction between these pathways in malignant *versus* normal tissue. However, it should be remembered that down-regulation of COX-2 by PPARγ was dependent on activation with PPARγ ligands, and it is not known whether the availability of endogenous ligands (*e.g.* certain polyunsaturated fatty acids as well as 15d-PGJ2) is different between normal and cancerous tissue. In addition, the fact that the activity of PPARγ is also dependent on its phosphorylation status (41) could provide another potential mechanism for the aberrant functioning of this receptor. Similar conflicting observations have also been reported in the case of colon cancer; that is high tissue expression of both PPARγ and COX-2, in the face of their inverse regulation by PPARγ and COX-2 activators (42). The cause(s) for the simultaneous high expression of PPARγ and COX-2 in colon cancer, as in cervical cancer, remains unknown.

In experiments to shed light on the mechanisms(s) responsible for the PPARγ-induced inhibition of COX-2 mRNA, electrophoretic mobility shift assays were performed to identify the binding activities in CaSki cells of the nuclear transcription factors AP-1 and NFκB. The human COX-2 promoter contains multiple transcription factor binding sites including NFκB, CRE, and NF-IL6. Recent reports demonstrated that AP-1 nuclear protein can bind to the CRE site located in the COX-2 promoter region in human mammary cells (31). Our results showing that CRE binding activity was attenuated in the presence of 100-fold excess of unlabeled AP-1 oligonucleotides demonstrated that this phenomenon is also true in cervical cancer cells. We showed that PPARγ ligand treatment of CaSki cervical cancer cells reduced the binding activities of both AP-1 and NFκB nuclear proteins. On the other hand, PPARγ ligands had little effect on AP-2, another transcription factor binding motif located in the COX-2 promoter, indicating that PPARγ signaling affects only certain transcription factors involved in COX-2 regulation. The blocking effect on AP-1 binding was inhibited in the presence of GW9662, a specific PPARγ antagonist, confirming that PPARγ signaling was involved in this activity. To determine whether these effects were responsible for PPARγ-mediated inhibition of COX-2, transient transfection experiments were performed with a series of COX-2 promoter reporter constructs in which the binding sites for NFκB and/or AP-1 nuclear protein were mutagenized. The results demonstrated that down-regulation of COX-2 by PPARγ ligands was predominantly mediated by antagonizing the transactivating activity of AP-1 nuclear proteins on the COX-2 promoter. This finding is consistent with that found in normal and malignant human mammary cells where this AP-1 binding to CRE site was shown to play a major role in mediating PPARγ ligand regulation of COX-2 expression (31). In contrast, it was found that modulation of COX-2 by PPARγ ligands in macrophages was largely mediated by NFκB (32). It is clear that regulation of COX-2 through PPARγ signaling is cell-type specific and may also be dependent on developmental processes.

The present data and previous findings have demonstrated that alteration of COX-2 levels can be mediated by a diverse group of seemingly unrelated natural, dietary, and synthetic compounds that have been shown to bind to and activate PPARγ (43–45). These include long chain PUFAs such as that found in fish oil (*e.g.* ω 3-PUFA), aromatic small chain fatty acids (*e.g.* phenylacetate), various eiconsanoids (*e.g.* 15d-PGJ2), lipid hydroperoxides [*e.g.* 9(s)-HODE], oxidatively modified lipoproteins (*e.g.* oxidized low-density lipoprotein), linoleic acid, thiazolidinediones (*e.g.* rosiglitazone), and a variety of recently synthesized compounds (*e.g.* GW1929). Studies in our laboratory have used a number of these agents in showing that 15d-PGJ2, GW1929, fish oil, and linoleic acid increased PPARγ while decreasing COX-2 mRNA levels. No differences have been seen between oleic acid, which is not a PPARγ ligand, and vehicle-treated control groups.[3] Because routine screening and diagnostic procedures for cervical cancer have become so well developed, this disease may represent the ideal cancer for chemopreventive intervention by dietary means or long-term pharmaceutical administration. As such, routine screening by Pap smear can detect dysplasia long before micro or frank invasive cancer develops. Thus, it is conceivable that dietary modification that includes high PPARγ ligand-containing foods might be able to prevent certain dysplastic progressions and cervical cancer occurrence. This hypothesis is supported by reports showing that populations having frequent intake of foods rich in ω 3 and ω 6 PUFA, such as found in boiled or broiled fish, show decreased risk of cervical cancer (46, 47).

In conclusion, our study indicates that there is cross-regulation between COX-2 and PPARγ gene expression in human cervical cancer cells. The ability of PPARγ ligands to inhibit COX-2 appears to be mediated predominantly through inhibi-

[3] Unpublished observations.

tion of AP-1 protein binding to the CRE binding site in the COX-2 promoter. Because COX-2 can act as a promoter of several cancers, the ability of PPARγ activators to inhibit COX-2 expression in human cervical cancer suggests that PPARγ signaling may be a useful target for therapeutic intervention and/or chemoprevention of this disease.

ACKNOWLEDGMENT

This work was supported by NIH grants CA85589 and HD35276.

REFERENCES

1. Smith, W. L., Garavito, R. M., and Dewitt, D. L. Prostaglandin endoperoxide H synthase (cyclooxygenase)-1 and -2. J. Biol. Chem., *271:* 33157–33160, 1996.

2. Soslow, R. A., Dannenberg, A. J., Rush, D., Woerner, B. M., Khan, K. N., Masferrer, J., and Koki, A. T. COX-2 is expressed in human pulmonary, colonic, and mammary tumors. Cancer (Phila.), *89:* 2637–2645, 2000.

3. Sjodahi, R., Nonsteroidal anti-inflammatory drugs and the gastrointestinal tract. Extent, mode, and dose dependence of anticancer effects. Am. J. Med., *110:* 66S–69S, 2001.

4. Kulkarni, S., Rader, J. S., Zhang, F., Liapis, H., Koki, A. T., Masferrer, J. L., Subbaramaiah, K., and Dannenberg, A. J. Cyclooxygenase-2 is overexpressed in human cervical cancer. Clin. Cancer Res., *7:* 429–434, 2001.

5. Greenlee, R. T., Murray, T., Bolden, S., and Wingo, P. A. Cancer statistics, 2000. CA Cancer J. Clin., *50:* 7–33, 2000.

6. Affney, D. K., Holden, J., Davis, M., Zempolich, K., Murphy, K. J., and Dodson, M. Elevated cyclooxygenase-2 expression correlates with diminished survival in carcinoma of the cervix treated with radiotherapy. Int. J. Radiat. Oncol. Biol. Phys., *49:* 1213–1217, 2001.

7. Mangelsdorf, D. J., Thummel, C., Beato, M., Herrlich, P., Schutz, G., Umesono, K., Blumberg, B., Kastner, P., Mark, M., Chambon, P., *et al.* The nuclear receptor superfamily: the second decade. Cell, *83:* 835–839, 1995.

8. Kersten, S., Desvergne, B., and Wahli, W. Roles of PPARs in health and disease. Nature (Lond.), *405:* 421–424, 2000.

9. Lemberger, T., Braissant, O., Juge-Aubry, C., Keller, H., Saladin, R., Staeles, B., Auwerx, J., Burger, A. G., Meier, C. A., and Wahli, W. PPAR tissue distribution and interactions with other hormone-signaling pathway. Ann. N. Y. Acad Sci., *804:* 231–251, 1996.

10. Braissant, O., Foufelle, F., Scotto, O., Dauca, M., and Wahli, W. Differential expression of peroxisome proliferator-activated receptor (PPARs) tissue distribution of PPAR-α, β, and –γ in the adult rat. Endocrinology, *137:* 354–366, 1996.

11. Richote, M., Huang, J. T., Welch, J. S., and Glass, C. K. The peroxisome proliferator-activated receptor γ (PPARγ) as a regulator of monocyte/macrophage function. J. Leukocyte. Biol.y, *66:* 733–739, 1999.

12. Nagy, L., Tontonoz, P., Alvarez, J. G., Chen, H., and Evans, R. M. Oxidized LDL regulates macrophage gene expression through ligand activation of PPARγ. Cell, *93:* 229–240, 1998.

13. Xu, H. E., Lambert, M. H., Montana, V. G., Parks, D. J., Blanchard, S. G., Brown, P. J. Sternbach, D. D., Lehmann, J. M., Wisely, G. B., Willson, T. M., Kliewer, S. A., and Milburn, M. V. Molecular recognition of fatty acids by peroxisome proliferator-activated receptors. Mol. Cell., *3:* 397–403, 1999.

14. Mansen, A., Guardiola-Biaz, H., Rafter, J., Branting, C., and Gustafsson, J-A., Expression of the peroxisome proliferator-activated receptor (PPAR) in the mouse colonic mucosa. Biochem. Biophy. Res. Commun., *222:* 844–851, 1996.

15. Xin, X., Yang, S., Kowalski, J., and Gerritsen, M. E. Peroxisome proliferator-activated receptor γ ligands are potent inhibitors of angiogenesis *in vitro* and *in vivo*. J. Biol. Chem., *274:* 9116–9121, 1999.

16. Chinery, R., Coffey, R. J., Graves-Deal, R., Kirkland, S. C., Sanchez, S. C., Zackert, W. E., Oates, J. A., and Morrow, J. D. Prostaglandin J2 and 15-deoxy-δ12, 14-prostaglandin J2 induce proliferation of cyclooxygenase-depleted colorectal cancer cells. Cancer Res., *59:* 2739–2746, 1999.

17. Meade, E. A., McIntyre, T. M., Zimmerman, G. A., and Prescott, S. M., Peroxisome proliferators enhance cyclooxygenase-2 expression in epithelial cells. J. Biol. Chem., *274:* 8328–8334, 1999.

18. Callejas, N. A., Castrillo, A., Bosca, L., and Martin-Sanz, P. Inhibition of prostaglandin synthesis up-regulates cyclooxygenase-2 induced by lipopolysaccharide and peroxisomal proliferators. J. Pharmacol. Exp. Ther., *288:* 1235–1241, 1999.

19. Sidell, N., Lucas, C. A., and Kreutzberg, G. W. Regualtion of acetylcholinesterase activity by retinoic acid in a human neuroblastoma cell line. Exp. Cell Res., *155:* 305–309, 1984.

20. Stacker, S. A., Runting, A. S., Caesar, C., Vitali, A., Lackmann, M., Chang, J., Ward, L., and Wilks, A. F. The 3T3–L1 fibroblast to adipocyte conversion is accompanied by increased expression of angiopoietin-1, a ligand for tie2. Growth Factors, *18:* 177–191, 2000.

21. Brown, K. K., Henke, B. R., Blanchard, S. G., Cobb, J. G., Mook, R., Kaldor, I., Kliewer, S. A., Lehmann, J. M., Lenhard, J. M., Harrington, W. W., Novak, P. J., Faison, W., Binz, J. G., Hashim, M. A., Oliver, O., Brown, H. R., Parks, D. J., Plunket, K. D., Tong, W. Q., Adkison, k., Noble, S. A., and Willson, T. M. A novel N-aryl Tyrosine activator of peroxisome proliferator-activated receptor-γ reverses the diabetic phenotype of zucker diabetic fatty rat. Diabetes, *48:* 1415–1424, 1999.

22. Miyahara, T., Schrum, L., Rippe, R., Xiong, S., Yee, H. F., Jr., Motomura, K., Anania, F. A., Willson, T. M., and Tsukamoto, H. Peroxisome proliferator-activated receptors and hepatic stellate cell activation. J. Biol. Chem., *275:* 35715–35722, 2000.

23. Futaki, N., Takahashi, S., Yokoyama, M., Arai, I., Higuchi, S., and Otomo, S. NS-398, a new anti-inflammatory agent, selectively inhibits prostaglandin G/H synthase/cyclooxygenase (COX-2) activity *in vitro*. Prostaglandins, *47:* 55–59, 1994.

24. Han, S., and Sidell, N. Peroxisome-proliferator-activated-receptor γ (PPARγ) independent induction of CD36 in THP-1 monocytes by retinoic acid. Immunology, *106:* 53–59, 2002.

25. Abassi, Z., Brodsky, S., Gealekman, O., Rubinstein, I., Hoffman, A., and Winaver, J. Intrarenal expression and distribution of cyclooxygenase isoforms in rats with experimental heart failure. Am. J. Physiol. Renal. Physiol., *280:* F43–53, 2001.

26. Dignam, J. D., Lebovitz, R. M., and Roeder, R. G. Accurate transcription initiation by RNA polymerase II in a soluble extract from isolated mammalian nuclei. Nucleic Acids Res., *11:* 1475–1489, 1983.

27. Inoue, H., Umesono, K., Nishimori, T., Hirata, Y., and Tanabe, T. Glucocorticoid-mediated suppression of the promoter activity of the cyclooxygenase-2 gene is modulated by expression of its receptor in vascular endothelial cells. Biochem. Biophys. Res. Commun., *254:* 292–298, 1999.

28. Han, S., Wada, R. K., and Sidell, N. Differentiation of human neuroblastoma by phenylacetate is mediated by peroxisome proliferator-activated receptor γ. Cancer Res., *61:* 3998–4002, 2001.

29. Tontonoz, P., Hu, E., and Spiegelman, B. M. Regulation of adipocyte gene expression and differentiation by peroxisome proliferator activated receptor γ. Curr. Opin. Genet. Dev., *5:* 571–576, 1995.

30. Fasshauer, M., Klein, J., Lossner, U., and Paschke, R. Isoproterenol is a positive regulator of the suppressor of cytokine signaling-3 gene expression in 3T3–L1 adipocytes. J. Endocrinol., *175:* 727–733, 2002.

31. Subbaramaiah, K., Lin, D. T., Hart, J. C., and Dannenberg, A. J., Peroxisome proliferator-activated receptor γ ligands suppress the transcriptional activation of cyclooxygenase-2. Evidence for involvement of activator protein-1 and CREB-binding protein/p300. J. Biol. Chem., *276:* 12440–12448, 2001.

32. Inoue, H., Tanabe, T., and Umesono, K. Feedback control of cyclooxygenase-2 expression through PPARγ. J. Biol. Chem., *275:* 28028–32802, 2000.

33. Howe, L. R., Subbaramaiah, K., Brown, A. M., and Dannenberg, A. J. Cyclooxygenase-2: a target for the prevention and treatment of breast cancer. Endocr. Relat. Cancer, *8:* 97–114, 2001.

34. Roberson, M. S., Ban, M., Zhang, T., and Mulvaney, J. M. Role of the cyclic AMP response element binding complex and activation of mitogen-activated protein kinases in synergistic activation of the glycoprotein hormone α subunit gene by epidermal growth factor and forskolin. Mol. Cell. Biol., *20:* 3331–344, 2001.

35. Zelenaia, O., Schlag, B. D., Gochenauer, G. E., Ganel, R., Song, W., Beesley, J. S., Grinspan, J. B., Rothstein, J. D., and Robinson, M. B. Epidermal growth factor receptor agonists increase expression of glutamate transporter GLT-1 inastrocytes through pathways dependent on phosphatidylinositol 3-kinase and transcription factor NF-κB. Mol. Pharmacol., *57:* 667–678, 2000.

36. Biswas, D. K., Cruz, A. P., Gansberger, E., and Pardee, A. B. Epidermal growth factor-induced nuclear factor κ B activation: a major pathway of cell-cycle progression in estrogen-receptor negative breast cancer cells. Proc. Natl. Acad. Sci. USA, *97:* 8542–8547, 2000.

37. Kirtikara, K., Raghow, R., Laulederkind, S. J., Goorha, S., Kanekura, T., and Ballou, L. R. Transcriptional regulation of cyclooxygenase-2 in the human microvascular endothelial cell line, HMEC-1: control by the combinatorial actions of AP2, NF-IL-6 and CRE elements. Mol. Cell. Biochem., *203:* 41–51, 2000.

38. Pontsler, A. V., St Hilaire, A., Marathe, G. K., Zimmerman, G. A., and McIntyre, T. M. Cyclooxygenase-2 is induced in monocytes by peroxisome proliferator activated receptor γ and oxidized alkyl phospholipids from oxidized low density lipoprotein. J. Biol. Chem., *277:* 13029–13036, 2002.

39. Kalajdzic, T., Faour, W. H., He, Q. W., Fahmi, H., Martel-Pelletier, J., Pelletier, J. P., and Di Battista, J. A. Nimesulide, a preferential cyclooxygenase 2 inhibitor, suppresses peroxisome proliferator-activated receptor induction of cyclooxygenase 2 gene expression in human synovial fibroblasts: evidence for receptor antagonism. Arthritis Rheum., *46:* 494–506, 2002.

40. Paik, J. H., Ju, J. H., Lee, J. Y., Boudreau, M. D., and Hwang, D. H. Two opposing effects of non-steroidal anti-inflammatory drugs on the expression of the inducible cyclooxygenase. Mediation through different signaling pathways. J. Biol. Chem., *275:* 28173–28179, 2000.

41. Hu, E. D., Kim, J. B., Sarraf, P., and Spiegelman, B. M. Inhibition of adipogenesis through MAP kinase-mediated phosphorylation of PPAR-γ. Science (Wash. DC), *274:* 2100–2103, 1996.

42. Yang, W. L., and Frucht, H. Activation of the PPAR pathway induces apoptosis and COX-2 inhibition in HT-29 human colon cancer cells. Carcinogenesis (Lond.), *22:* 1379–1383, 2001.

43. Aronson, W. J., Glaspy, J. A., Reddy, S. T., Reese, D., Heber, D., and Bagga, D. Modulation of omega-3/omega-6 polyunsaturated ratios with dietary fish oils in men with prostate cancer. Urology, *58:* 283–288, 2001.

44. Pontsler, A. V., St Hilaire, A., Marathe, G. K., Zimmerman, G. A., and McIntyre, T. M. Cyclooxygenase-2 is induced in monocytes by peroxisome proliferator activated receptor γ and oxidized alkyl phospholipids from oxidized low density lipoprotein. J. Biol. Chem., *277:* 13029–36, 2002.

45. Krey, G., Braissant, O., L'Horset, F., Kalkhoven, E., Perroud, M., Parker, M. G., and Wahli, W. Fatty acids, eicosanoids, and hypolipidemic agents identified as ligands of peroxisome proliferator-activated receptors by coactivator-dependent receptor ligand assay. Mol. Endocrinol., *11:* 779–791, 1997.

46. Hirose, K., Tajima, K., Hamajima, N., Takezaki, T., Inoue, M., Kuroishi, T., Kuzuya, K., Nakamura, S., and Tokudome, S. Subsite (cervix/endometrium)-specific risk and protective factors in uterus cancer. Jpn. J. Cancer Res., *87:* 1001–1009, 1996.

47. Hursting, S. D., Thornquist, M., and Henderson, M. M. Types of dietary fat and the incidence of cancer at five sites. Prev. Med., *19:* 242–253, 1990.

ELSEVIER

Neuroscience Letters 352 (2003) 203–206

Neuroscience Letters

www.elsevier.com/locate/neulet

Brain protection by resveratrol and fenofibrate against stroke requires peroxisome proliferator-activated receptor α in mice

Hiroyasu Inoue[a], Xiao-Fan Jiang[b], Takahiro Katayama[b], Shiho Osada[c], Kazuhiko Umesono[c,†], Shobu Namura[b,d,*]

[a]*Department of Pharmacology, National Cardiovascular Center Research Institute, 5-7-1 Fujishirodai, Suita, Osaka 565-8565, Japan*
[b]*Stroke and Brain Protection Laboratory, National Cardiovascular Center Research Institute, 5-7-1 Fujishirodai, Suita, Osaka 565-8565, Japan*
[c]*Department of Molecular Biology and Genetics, Institute for Virus Research, Kyoto University, Shogoin Kawaharacho, Sakyoku, Kyoto 606-8397, Japan*
[d]*Department of Neurological Surgery, Cerebrovascular Research Center, Cleveland Clinic Foundation NB20, 9500 Euclid Avenue, Cleveland, OH 44195, USA*

Received 4 August 2003; received in revised form 29 August 2003; accepted 1 September 2003

Abstract

Peroxisome proliferator-activated receptors (PPARs) are ligand-dependent transcription factors which belong to the nuclear receptor family. We examined whether PPARα agonists and resveratrol, a polyphenol contained in grapes, protect the brain against ischemia. To investigate whether resveratrol activates PPARs, we performed a cell-based transfection activity assay using luciferase reporter plasmid. PPARα and PPARγ were activated by resveratrol in primary cortical cultures and vascular endothelial cells. Resveratrol (20 mg/kg, 3 days) reduced infarct volume by 36% at 24 h after middle cerebral artery occlusion in wild-type mice. The PPARα agonists fenofibrate (30 mg/kg, 3 days) and Wy-14643 (30 mg/kg, 7 days) exerted similar brain protection. However, resveratrol and fenofibrate failed to protect the brain in PPARα knockout mice. The data indicate that PPARα agonists protect the brain through PPARα.

Keywords: Nuclear receptor; Peroxisome proliferator activated receptor; Polyphenol; Inflammation; Focal cerebral ischemia; Neuroprotection; Mouse

Peroxisome proliferator-activated receptors (PPARs) are members of the nuclear hormone receptor family of ligand-dependent transcription factors [17]. PPARs form heterodimers with the 9-*cis* retinoic acid receptor RXR, binding to specific peroxisome proliferator responsive elements (PPREs) in the promoter regions of specific target genes. The PPAR subfamily comprises of three isotypes: PPARα, PPARβ (also called PPARδ, NUC-1 or FAAR), and PPARγ. Although a precise biological role for PPARβ remains unclear, PPARα and PPARγ play a key role in the metabolism of lipids and glucose [1,17]. For example, hypolipidemic compounds of the fibrate class, including Wy-14643 and clofibrate, activate PPARα [10]. The thiazolidinediones (TZDs), which were originally identified as insulin-sensitizing agents to treat type II diabetes, bind selectively to PPARγ [11].

PPARα and PPARγ have been implicated in inflammation: for example, PPARα and PPARγ exert anti-inflammatory effects [7,13,16]. Fibrates, PPARα ligands, exert anti-inflammatory actions by antagonizing nuclear factor (NF)-κB in aortic smooth muscle cells [16]. Similarly, TZDs and 15-deoxy-$\Delta^{12,14}$prostaglandin J_2 (15-deoxy-PGJ_2), a potential endogenous PPARγ ligand, inhibit both macrophage activation and production of pro-inflammatory molecules [7,13]. Since ligands of PPARα and PPARγ reduce myocardial infarct size [14,19,20], PPARα and PPARγ may also constitute a potential target for the development of anti-ischemic drugs.

Resveratrol, a polyphenol abundantly found in the skin and seeds of grapes [15], has anti-inflammatory activity similar to PPAR agonists [8]. Resveratrol inhibits platelet aggregation, promotes vasodilation, and exerts anti-atherosclerotic effects [3]. Moreover, resveratrol has been shown to protect organs such as heart, brain, and kidney against ischemia/reperfusion [4,12]. Thus, PPARs ligands and resveratrol share a great similarity in their biological

* Corresponding author (address d). Tel.: +1-216-445-0563; fax: +1-216-445-1466.
E-mail address: namuras@ccf.org (S. Namura).
† Deceased.

0304-3940/03/$ - see front matter © 2003 Elsevier Ireland Ltd. All rights reserved.
doi:10.1016/S0304-3940(03)01080-2

actions. We hypothesized that a link exists between nuclear receptors and resveratrol. Interactions of resveratrol with nuclear receptors were also suggested by the data that glucocorticoids [6], 15-deoxy-PGJ_2 [5], and resveratrol (unpublished data) suppress the lipopolysaccharide (LPS)-induced expression of cyclooxygenase-2 (COX-2) mRNA in U937 cells.

To examine whether resveratrol activates nuclear receptors, we employed a cell-based transfection assay in monkey kidney CV-1 cells using the ligand binding domain of nuclear receptors fused to the DNA-binding domain of the yeast transcription factor GAL4 [18]. The CV-1 cells were transfected for 6 h, washed, and incubated with resveratrol for 40 h. Resveratrol activated the nuclear receptors PPARα and PPARγ in a dose-dependent manner (Fig. 1A). In contrast, resveratrol did not activate other nuclear receptors including glucocorticoid receptor (GR) and PPARδ even at 100 μM (Fig. 1B). Thus, these data indicate that resveratrol is a selective activator of PPARα and PPARγ.

Next, we examined whether the activation of PPARα and PPARγ by resveratrol can be induced in mouse primary cortical cultures and bovine brain microvessel vascular endothelial cells (BBMEC). To test this, we transfected a reporter vector of PPRE with the expression vector for PPARα or PPARγ. Mouse primary cortical cultures and BBMEC were transfected as described [5]. The transfection mixtures in each well contained 0.15 μg of tk-PPREx3-Luc reporter plasmid, 0.15 μg of pCMX-mPPARα or pCMX-mPPARγ, and 0.02 μg of pSV-βgal. Cortical cultures were incubated with the transfection mixtures for 16 h. BBMEC were incubated with the transfection mixtures for 4 h. Luciferase activity was standardized by the β-galactosidase activity. Treatment with 10 μM resveratrol for 24 h activated PPARα and PPARγ in both cell types (Fig. 2). Comparable activation of PPARα and PPARγ by resveratrol was also found in human umbilical venous endothelial cells (HUVEC) and bovine arterial endothelial cells (BAEC) (Fig. 2).

Resveratrol has been shown to be neuroprotective [4]. We examined whether resveratrol is beneficial against cerebral ischemia in a mouse experimental stroke model. Resveratrol was given orally, and mice were subjected to permanent middle cerebral artery occlusion (MCAO) under 1% halothane anesthesia. Brain infarct area was assessed on coronal sections stained with 2% 2,3,5-triphenyltetrazolium chloride at 24 h after onset of MCAO. Single administration of resveratrol at 1 h before MCAO did not exert detectable brain protection (Fig. 3A); however, daily administrations

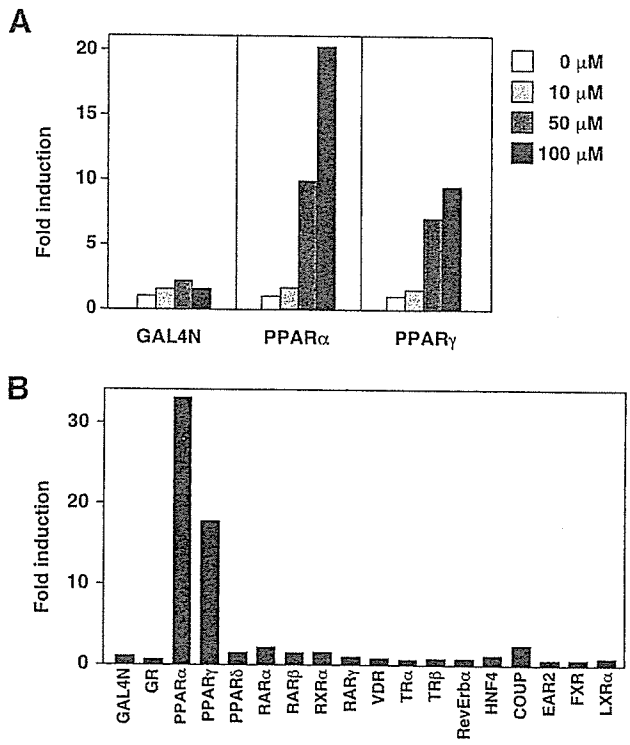

Fig. 1. Resveratrol is a selective activator of PPARα and PPARγ. (A) Dose-dependent activation of GAL4-PPAR ligand binding domain chimeras by resveratrol in transiently transfected CV-1 cells. (B) Activation of GAL4-nuclear receptor ligand binding domain chimeras by 100 μM resveratrol in CV-1 cells. Data were collected from two independent experiments, and presented as means. GAL4N, yeast GAL4 DNA binding domain; GR, glucocorticoid receptor; RAR, retinoic acid receptor; RXR, retinoid X receptor; VDR, vitamin D receptor; TR, thyroid hormone receptor; RevErb, Rev-ErbA α; HNF, hepatocyte nuclear factor; COUP, chicken ovalbumin upstream promoter transcription factor; EAR2, v-Erb-A avian erythroblastic leukemia viral oncogene homolog-like 2; FXR, farnesoid X receptor; LXR, liver X receptor.

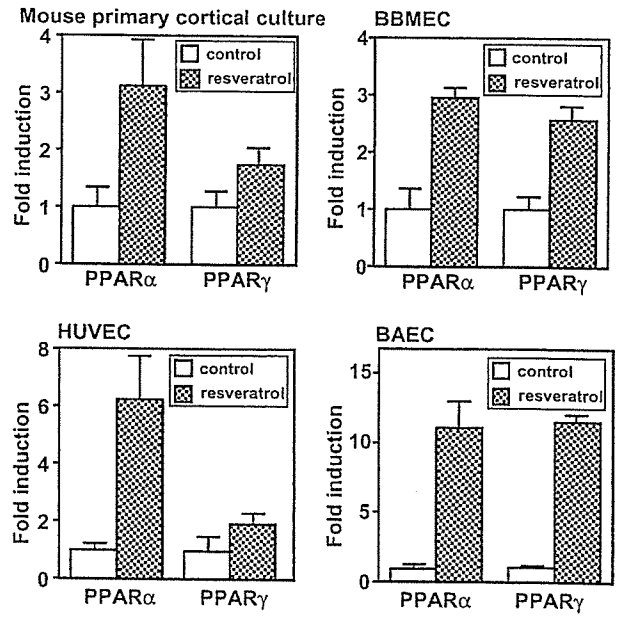

Fig. 2. Resveratrol activates PPRE in murine primary cortical cultures, bovine brain microvessel vascular endothelial cells (BBMEC), human umbilical venous endothelial cells (HUVEC) and bovine arterial endothelial cells (BAEC). Cells were cotransfected with expression plasmids encoding either PPARα or PPARγ and the reporter plasmid tk-PPREx3-Luc and incubated in the presence or absence of 10 μM resveratrol for 24 h. Data were collected from three independent experiments, and presented as mean ± standard deviation. Statistical analysis was made by Student's *t*-test.

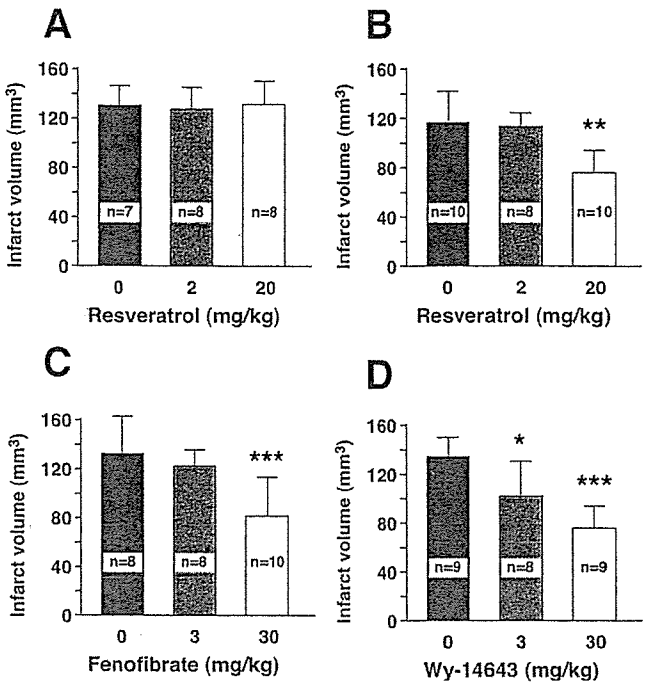

Fig. 3. Resveratrol and PPARα ligands attenuate brain infarct in a mouse stroke model. (A) Infarct volume at 24 h after MCAO in ddY mice treated with resveratrol at 1 h before MCAO. (B) Infarct volume at 24 h after MCAO in ddY mice treated with resveratrol for 3 days. $^{**}P < 0.01$ compared with 0 mg/kg. (C) Infarct volume at 24 h after MCAO in ddY mice treated with fenofibrate for 3 days. $^{***}P < 0.001$ compared with 0 mg/kg. (D) Infarct volume at 24 h after MCAO in ddY mice treated with Wy-14643 for 7 days. $^{*}P < 0.05$, $^{***}P < 0.001$ compared with 0 mg/kg. Data are presented as mean ± standard deviation, and statistical comparison was made by analysis of variance followed by Scheffe's test.

(20 mg/kg) for 3 days significantly reduced infarct size by 36% (Fig. 3B). Resveratrol treatment for 3 days did not affect serum levels of cholesterol and triglycerides, or body temperature (data not shown).

We also examined the effects of fenofibrate and Wy-14643, both of which are ligands of PPARα [10]. Daily oral administrations of fenofibrate (30 mg/kg for 3 days) and Wy-14643 (30 mg/kg for 7 days) significantly reduced infarct size by 34% and 44% compared with vehicle, respectively (Fig. 3C,D). Together with our findings that resveratrol activates PPARα, these data suggested that the protective effect of resveratrol is mediated through PPARα.

Finally, to examine whether PPARα expression is required for brain protection by resveratrol and fibrates, we tested resveratrol or fenofibrate in PPARα knockout mice [9]. PPARα knockout mice did not show detectable protection by either resveratrol or fenofibrate (Fig. 4), indicating a critical role for PPARα in the brain protection by PPARα agonists.

The current study herein demonstrated three major findings. First, resveratrol is a dual activator of the PPARα and PPARγ. Second, pretreatment with the ligands of PPARα, fenofibrate and Wy-14643, reduced brain infarct size after permanent focal cerebral ischemia, similar to what shown after pretreatment with resveratrol. Third, resveratrol

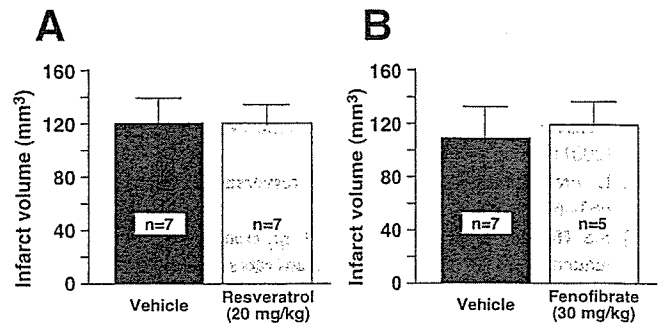

Fig. 4. Resveratrol and fenofibrate do not attenuate brain infarct in PPARα knockout mice. (A) Infarct volume at 24 h after MCAO in PPARα knockout mice treated with resveratrol (20 mg/kg) for 3 days. (B) Infarct volume at 24 h after MCAO in PPARα knockout mice treated with fenofibrate (30 mg/kg) for 3 days. Data are presented as mean ± standard deviation. There is no statistical difference between the groups (Student's *t*-test).

and fenofibrate failed to protect against cerebral ischemia in PPARα gene knockout mice. Thus, resveratrol and fenofibrate require PPARα expression to exert brain protection against permanent focal cerebral ischemia. The present data suggest that PPARα may be a potential target for developing drugs for stroke. This notion is supported by the recent clinical evidence that gemfibrozil reduces stroke incidence in patients with coronary heart disease [2].

How PPARα agonists protect brain remains to be studied. Resveratrol was not protective in PPARα knockout mice, which suggests that a direct free radical scavenging action of resveratrol may not be the mode of protection in this mouse permanent ischemia model. Agonists of PPARα and PPARγ have recently been demonstrated to reduce myocardial infarct size in rat heart ischemia/reperfusion models [14,19,20]. These effects appear to be related with their anti-inflammatory actions. Together with the hypolipidemic, anti-diabetic, and anti-inflammatory effects of agonists of PPARα and PPARγ, PPARs may be potential targets for developing anti-ischemic drugs.

Acknowledgements

We thank Dr M. Mayberg and Dr D. Janigro for critical reading and comments on the manuscript. This work was supported by grants from the Ministry of Education, Science, Sports, Culture and Technology of Japan; the Ministry of Health, Welfare, and Labor of Japan; Yamanouchi USA Foundation; and CCF-Cerebrovascular Research Bridge Program. This paper is dedicated to the memory of K.U.

References

[1] Y. Barak, M.C. Nelson, E.S. Ong, Y.Z. Jones, P. Ruiz-Lozano, K.R. Chien, A. Koder, R.M. Evans, PPAR gamma is required for placental, cardiac, and adipose tissue development, Mol. Cell 4 (1999) 585–595.

[2] H. Bloomfield Rubins, J. Davenport, V. Babikian, L.M. Brass, D. Collins, L. Wexler, S. Wagner, V. Papademetriou, G. Rutan, S.J. Robins, VA-HIT Study Group. Reduction in stroke with gemfibrozil in men with coronary heart disease and low HDL cholesterol: The Veterans Affairs HDL Intervention Trial (VA-HIT), Circulation 103 (2001) 2828–2833.
[3] L. Frémont, Biological effects of resveratrol, Life Sci. 66 (2000) 663–673.
[4] S.S. Huang, M.C. Tsai, C.L. Chih, L.M. Hung, S.K. Tsai, Resveratrol reduction of infarct size in Long-Evans rats subjected to focal cerebral ischemia, Life Sci. 69 (2001) 1057–1065.
[5] H. Inoue, T. Tanabe, K. Umesono, Feedback control of cyclooxygenase-2 expression through PPARγ, J. Biol. Chem. 275 (2000) 28028–28032.
[6] H. Inoue, K. Umesono, T. Nishimori, Y. Hirata, T. Tanabe, Glucocorticoid-mediated suppression of the promoter activity of the cyclooxygenase-2 gene is modulated by expression of its receptor in vascular endothelial cells, Biophys. Biophys. Res. Commun. 254 (1999) 292–298.
[7] C. Jiang, A.T. Ting, B. Seed, PPAR-γ agonists inhibit production of monocyte inflammatory cytokines, Nature 391 (1998) 82–86.
[8] Y. Kimura, H. Okuda, S. Arichi, Effects of stilbenes on arachidonate metabolism in leukocytes, Biochim. Biophys. Acta 834 (1985) 275–278.
[9] S.S.-T. Lee, T. Pineau, J. Drago, E.J. Lee, J.W. Owens, D.L. Kroetz, P.M. Fernandez-Salguero, H. Westphal, F.J. Gonzalez, Targeted disruption of the α isoform of the peroxisome proliferator-activated receptor gene in mice results in abolishment of the pleiotropic effects of peroxisome proliferators, Mol. Cell. Biol. 15 (1995) 3012–3022.
[10] J.M. Lehmann, J.M. Lenhard, B.B. Oliver, G.M. Ringold, S.A. Kliewer, Peroxisome proliferator-activated receptors alpha and gamma are activated by indomethacin and other non-steroidal anti-inflammatory drugs, J. Biol. Chem. 272 (1997) 3406–3410.
[11] J.M. Lehmann, L.B. Moore, T.A. Smith-Oliver, W.O. Wilkison, T.M. Willson, S.A. Kliewer, An antidiabetic thiazolidinedione is a high affinity ligand for peroxisome proliferator-activated receptor gamma (PPAR γ), J. Biol. Chem. 270 (1995) 12953–12956.
[12] P.S. Ray, G. Maulik, G.A. Cordis, A.A. Bertelli, A. Bertelli, D.K. Das, The red wine antioxidant resveratrol protects isolated rat hearts from ischemia reperfusion injury, Free Radic. Biol. Med. 27 (1999) 160–169.
[13] M. Ricote, A.C. Li, T.M. Willson, C.J. Kelly, C.K. Glass, The peroxisome proliferator-activated receptor-γ is a negative regulator of macrophage activation, Nature 391 (1998) 79–82.
[14] T. Shiomi, H. Tsutsui, S. Hayashidani, N. Suematsu, M. Ikeuchi, J. Wen, M. Ishibashi, T. Kubota, K. Egashira, A. Takeshita, Pioglitazone, a peroxisome proliferator-activated receptor-gamma agonist, attenuates left ventricular remodeling and failure after experimental myocardial infarction, Circulation 106 (2002) 3126–3132.
[15] G.J. Soleas, E.P. Diamandis, D.M. Goldberg, Wine as a biological fluid: history, production, and role in disease prevention, J. Clin. Lab. Anal. 11 (1997) 287–313.
[16] B. Staels, W. Koenig, A. Habib, R. Merval, M. Lebret, I.P. Torra, P. Delerive, A. Fadel, G. Chinetti, J.C. Fruchart, J. Najib, J. Maclouf, A. Tedgui, Activation of human aortic smooth-muscle cells is inhibited by PPARα but not by PPARγ activators, Nature 393 (1998) 790–793.
[17] I.P. Torra, G. Chinetti, C. Duval, J.C. Fruchart, B. Staels, Peroxisome proliferator-activated receptors: from transcriptional control to clinical practice, Curr. Opin. Lipidol. 12 (2001) 245–254.
[18] K. Umesono, R.M. Evans, Determinants of target gene specificity for steroid/thyroid hormone receptors, Cell 57 (1989) 1139–1146.
[19] N.S. Wayman, Y. Hattori, M.C. McDonald, H. Mota-Filipe, S. Cuzzocrea, B. Pisano, P.K. Chatterjee, C. Thiemermann, Ligands of the peroxisome proliferator-activated receptors (PPAR-gamma and PPAR-alpha) reduce myocardial infarct size, FASEB J. 16 (2002) 1027–1040.
[20] T.L. Yue, J. Chen, W. Bao, P.K. Narayanan, A. Bril, W. Jiang, P.G. Lysko, J.L. Gu, R. Boyce, D.M. Zimmerman, T.K. Hart, R.E. Buckingham, E.H. Ohlstein, In vivo myocardial protection from ischemia/reperfusion injury by the peroxisome proliferator-activated receptor-γ agonist rosiglitazone, Circulation 104 (2001) 2588–2594.

Chapter #29

INDUCTION OF CYCLOOXYGENASE-2 EXPRESSION BY FLUID SHEAR STRESS IN VASCULAR ENDOTHELIAL CELLS

Hiroyasu Inoue, Yoji Taba, Yoshikazu Miwa, Chiaki Yokota, Megumi Miyagi, and Toshiyuki Sasaguri

Introduction

Vascular endothelial cells are exposed to a wide variety of biomechanical stimuli including fluid shear stress caused by blood flow. Shear stress modulates several endothelial functions, such as control of vascular tone, maintenance of antithrombotic surfaces, regulation of inflammation, protection against oxidative stresses, and regulation of endothelial cell proliferation and apoptosis.

Cyclooxygenase (COX), a rate-limiting enzyme for prostaglandin (PG) biosynthesis, comprises two isozymes, COX-1 and COX-2. Laminar shear stress upregulates COX-2 gene expression [1-3]. We found that COX-2 is involved in lipopolysaccharide (LPS)-stimulated production of prostacyclin (PGI_2) in endothelial cells [4]. And that, shear stress promotes the production of PGD_2 in endothelial cells by stimulating the expression of lipocalin-type PGD_2 synthase (L-PGDS), whereas PGI_2 synthase is constitutively expressed in the presence or absence of the shear stress [5]. Therefore, it is necessary to evaluate the roles of COX-2 and L-PGDS expression by shear stress, which will be distinctly involved in the production of PGI_2 and PGD_2 in endothelial cells.

Three cis-acting elements, namely the NF-κB binding site, NF-IL6 binding site, and cyclic AMP response element, reside in the region between base pairs -327 and +59 (-327/+59) in the human COX-2 gene promoter. Their involvement in COX-2 gene transcription varies among cell species [6]. Recently, the COX-2 gene has been reported to be post-transcriptionally regulated through its 3'-untranslated region (3'-UTR) containing 17 copies

of the "AUUUA" motif, which is assumed to promote mRNA degradation. However, the mechanism underlying shear stress-induced COX-2 gene expression remains to be elucidated.

We investigated the molecular mechanism for the shear stress-induced expression of COX-2 in vascular endothelial cells. The gene expression of COX-2 was more sensitive to shear strength than that of L-PGDS. We found that shear stress induces COX-2 expression not only at the transcriptional level but also at the post-transcriptional level through the 3'-UTR, which would make it possible to rapidly and persistently induce COX-2 expression in response to shear stress [7].

Materials And Methods

Materials and experimental procedures have been described in detail elsewhere [4-7].

Results and Discussions

Exposure of human umbilical vein endothelial cells (HUVECs) to laminar shear stress in the physiological range (1 to 30 dyne/cm^2) upregulated the expression of cyclooxygenase (COX) -2 but not COX-1. The expression of COX-2 mRNA began to increase within 0.5 hours after the loading of the shear stress and reached a maximal level at 4 hours, which was more sensitive to shear strength than that of L-PGDS. (Table 1)

Table 1.Comparison of induction of COX-2 and L-PGDS mRNAs by fluid shear stress

Shear stress	Induction of COX-2[7]	Induction of L-PGDS[5]
Lower shear stress (1 dyne/cm^2)	Yes	No
Higher shear stress (15 dyne/cm^2)	Yes Rapid (within 30 min) Maximal level at 4 hours	Yes Time-lag (6 hours) Maximal level at 18 hours

Roles of the promoter region and the 3'-UTR in the human COX-2 gene were evaluated by the transient transfection of luciferase (Luc) reporter vectors into bovine arterial endothelial cells. Shear stress elevated Luc activity via the region (-327/+59 bp) in the COX-2 promoter. Mutation analysis indicated that cAMP responsive element (-59/-53 bp) was mainly involved in the shear stress-induced COX-2 expression. Moreover, shear stress selectively stabilized COX-2 mRNA in HUVECs. When a 3'-UTR containing 17 copies of the AUUUA mRNA instability motif was inserted into downstream of the Luc coding region, shear stress elevated the Luc expression. These results suggested that transcriptional activation and post-

transcriptional mRNA stabilization both contribute to the rapid and sustained expression of COX-2 in response to shear stress. Taken these findings together, COX-2 but not COX-1 will be mainly involved in PGI_2 formation in blood vessels loaded with laminar shear stress in the physiological range. This assumption is consistent with recent reports as follows.

1) Selective COX-2 inhibitors suppress the systemic biosynthesis of PGI_2 in healthy humans [8].

2) Glucocorticoids do not depress excretion of urinary PGI_2 metabolite [9].

3) COX-2 expression is involved in PGI_2 formation, but is not suppressed by dexamethasone in vascular endothelial cells [4].

4) COX-2 preferentially cooperates with PGI_2 synthase more than COX-1 [10].

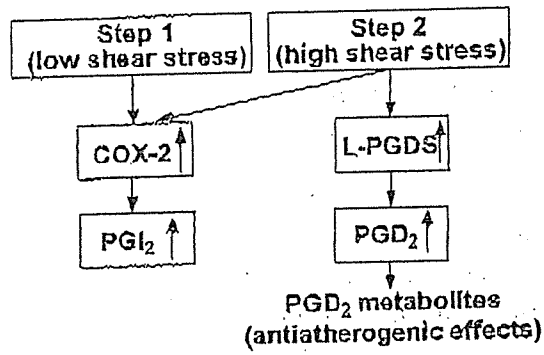

Figure 1. Possible roles of COX-2 and L-PGDS in endothelial cells

Concerning distinct regulation of COX-2 and L-PGDS expression by fluid shear stress, we hypothesize that there are two steps in COX-2-mediated arachidonate metabolism in endothelial cells (Figure 1). In this context, PGD_2 may also play a role in preventing the formation of atherosclerotic lesions by being converted to 15-deoxy-$\Delta^{12,14}$-PGJ_2, which has been reported to display several antiatherogenic effects on cultured vascular cells [11].

Macrophages were reported to express augmented levels of COX-2 in atherosclerotic lesions. This abnormally elevated COX-2 expression in macrophages may be related with inflammation in the lesions. Since the PGs produced in macrophages are different from those produced in endothelial cells, the regulation of COX-2 and downstream enzymes should be different between endothelial cells and macrophages. In this context, we have reported that COX-2 expression is negatively regulated by nuclear receptor PPARγ and its ligand candidate 15-deoxy-$\Delta^{12,14}$-PGJ_2 in macrophages but not in endothelial cells [6]. It should be examined whether changes in the pattern of blood flow, such as turbulence, influence the PG species produced in the cardiovascular system.

Acknowledgements

This study was partly supported by grants from the Ministry of Education, Science, Sports and Culture, Japan (a Grant-in-Aid for Scientific Research 11838021 and 13670110), and from the Ministry of Health and Welfare, Japan (Research Grants for Cardiovascular Diseases 11C-1 and 12C-3).

References

1. Topper JN, Cai J, Falb D, Gimbrone MA Jr. Identification of vascular endothelial genes differentially responsive to fluid mechanical stimuli. Proc Natl Acad Sci USA 1996; 93:10417-10422.
2. Okahara K, Sun B, Kambayashi J. Arterioscler Thromb Vasc Biol Upregulation of prostacyclin synthesis-related gene expression by shear stress in vascular endothelial cells. 1998; 18:1922-1926.
3. Ogasawara A, Arakawa, T, Kaneda T, Takuma T, Sato T, Kaneko H, Kumegawa M, Hakeda Y. Fluid shear stress-induced cyclooxygenase-2 expression is mediated by C/EBPβ, cAMP-response element-binding protein, and AP-1 in osteoblastic MC3T3-E1 cells. J Biol Chem 2001; 276:7048-7054.
4. Inoue H, Umesono K, Nishimori T, Hirata Y, Tanabe T. Glucocorticoid-mediated suppression of the promoter activity of the cyclooxygenase-2 gene is modulated by expression of its receptor in vascular endothelial cells. Biochem Biophys Res Commun 1999; 254:292-298.
5. Taba Y, Sasaguri T, Miyagi M, Abumiya T, Miwa Y, Ikeda T, Mitsumata M. Fluid shear stress induces lipocalin-type prostaglandin D_2 synthase expression in vascular endothelial cells. Circ Res 2000; 86:967-973.
6. Inoue H, Tanabe T, Umesono K. Feedback control of cyclooxygenase-2 expression through PPARγ. J Biol Chem. 2000; 275: 28028-28032.
7. Inoue H, Taba Y, Miwa Y, Yokota C, Miyagi M, Sasaguri T. Transcriptional and posttranscriptional regulation of cyclooxygenase-2 expression by fluid shear stress in vascular endothelial cells. Arterioscler Thromb Vasc Biol 2002; 22:1415-1420.
8. McAdam BF, Catella-Lawson F, Mardini IA, Kapoor S, Lawson JA, FitzGerald GA. Systemic biosynthesis of prostacyclin by cyclooxygenase (COX)-2. Proc Natl Acad Sci USA 1999;96: 272-277.
9. Sebaldt RJ, Sheller JR, Oates, JA, Roberts II LJ, FitzGerald GA. Inhibition of eicosanoid biosynthesis by glucocorticoids in humans. Proc Natl Acad Sci USA 1990; 87:6974-6978
10. Ueno N, Murakami M, Tanioka T, Fujimori K, Tanabe T, Urade Y, Kudo I. Coupling between cyclooxygenase, terminal prostanoid synthase, and phospholipase A2. J Biol Chem 2001; 276:34918-34927.
11. Miwa Y, Sasaguri T, Inoue H, Taba Y, Ishida A, Abumiya T. 15-deoxy-$\Delta^{12,14}$-prostaglandin J_2 induces G_1 arrest and differentiation marker expression in vascular smooth muscle cells. Mol Pharmacol 2000; 58:837-844.

Journal of the American College of Cardiology
© 2003 by the American College of Cardiology Foundation
Published by Elsevier Science Inc.

Vol. 41, No. 6, 2003
ISSN 0735-1097/03/$30.00
doi:10.1016/S0735-1097(02)03007-3

Biodegradable Gelatin Hydrogel Potentiates the Angiogenic Effect of Fibroblast Growth Factor 4 Plasmid in Rabbit Hindlimb Ischemia

Hirofumi Kasahara, MD,* Etsuro Tanaka, MD, PHD,†§ Naoto Fukuyama, MD, PHD,†§ Eriko Sato, MD,* Hiromi Sakamoto, PHD,‖ Yasuhiko Tabata, PHD,¶ Kiyoshi Ando, MD, PHD,‡§ Harukazu Iseki, MD, PHD,‡ Yoshiro Shinozaki, BS,† Koji Kimura, MD,* Eriko Kuwabara, MD,* Shirosaku Koide, MD, PHD,* Hiroe Nakazawa, MD, PHD,† Hidezo Mori, MD, PHD#

Isehara, Tokyo, Kyoto, and Suita, Japan

OBJECTIVES We investigated the potentiation of gene therapy using fibroblast growth factor 4 (FGF4)-gene by combining plasmid deoxyribonucleic acid (DNA) with biodegradable gelatin hydrogel (GHG).

BACKGROUND Virus vectors transfer genes efficiently but are biohazardous, whereas naked DNA is safer but less efficient. Deoxyribonucleic acid charges negatively; GHG has a positively charged structure and is biodegradable and implantable; FGF4 has an angiogenic ability.

METHODS The GHG-DNA complex was injected into the hindlimb muscle (63 mice and 55 rabbits). Gene degradation was evaluated by using ^{125}I-labeled GHG-DNA complex in mice. Transfection efficiency was evaluated with reverse-transcription nested polymerase chain reaction and X-Gal histostaining. The therapeutic effects of GHG-FGF4-gene complex (GHG-FGF4) were evaluated in rabbits with hindlimb ischemia.

RESULTS Gelatin hydrogel maintained plasmid in its structure, extending gene degradation temporally until 28 days after intramuscular delivery, and improving transfection efficiency. Four weeks after gene transfer, hindlimb muscle necrosis was ameliorated more markedly in the GHG-FGF4 group than in the naked FGF4-gene and GHG-beta-galactosidase (control) groups ($p < 0.05$, Kruskal-Wallis test). Synchrotron radiation microangiography (spatial resolution, 20 μm) and flow determination with microspheres confirmed significant vascular responsiveness to adenosine administration in the GHG-FGF4 group, but not in the naked FGF4-gene and the control.

CONCLUSIONS The GHG-FGF4 complex promoted angiogenesis and blood flow regulation of the newly developed vessels possibly by extending gene degradation and improving transfection efficiency without the biohazard associated with viral vectors. (J Am Coll Cardiol 2003;41: 1056–62) © 2003 by the American College of Cardiology Foundation

Angiogenic gene therapy using growth factors is widely studied to treat ischemic heart disease and severe limb ischemia (1,2). Of the two major methods of gene transfer, the use of virus vectors is efficient but biohazardous (3,4), while naked deoxyribonucleic acid (DNA) is safer, but less efficient (5). A highly efficient and safe drug delivery system without using a virus vector is needed for gene therapy in humans. We developed a new hydrogel consisting of amino acids, being biodegradable and, therefore, implantable, from gelatin (6). Hydrogel has been used to improve transfection efficiency in a hydrogel-coated balloon catheter (7). However, this hydrogel was not implantable because it consisted of carbohydrate and was not biodegradable. The purpose of the present study is to assess whether biodegradable gelatin hydrogel (GHG) improves the efficacy of gene therapy with the fibroblast growth factor 4 (FGF4)/hst1 gene; FGF4 is a growth factor discovered in human gastric cancer (8) and has a secretion signal domain (9). Its angiogenic ability has been confirmed both in vitro and in vivo (10).

METHODS

Experimental animals. All animal experiments were performed in accordance under the Guidelines of Tokai University School of Medicine on Animal Use, which conform to the National Institute of Health (NIH) Guide for the Care and Use of Laboratory Animals, DHEW publication No. (NIH) 86-23, revised 1985, Offices of Science and Health Reports, DRR/NIH, Bethesda, Maryland. Fifty-five Japanese white rabbits weighting 2.45 to 2.85 kg (Nihon Nosan Co., Tokyo, Japan) of both genders were used. The animals were anesthetized by intravenous injection of sodium pentobarbital (40 mg/kg), and hindlimb ischemia was created by the method of Takeshita et al. (11). Sixty-three

From the Departments of *Cardiovascular Surgery, †Physiology, ‡Internal Medicine, and §Research Center for Genetic Engineering and Cell Transplantation, Tokai University School of Medicine, Isehara, Japan; ‖Genetics Division, National Cancer Center Research Institute, Tokyo, Japan; ¶Research Center for Biomedical Engineering, Kyoto University, Kyoto, Japan; #Department of Cardiac Physiology, National Cardiovascular Center Research Institute, Suita, Japan. Supported by Grants-in-Aid for Scientific Research (13470154, 13470381, 13877114, 14657460, 14657461) from the MECSST; New Energy and Industrial Technology Development Organization; The Science Frontier Program of MESSC; The Research Grants for Cardiovascular Disease (H13C-1) and for Cancer Research (9-3, 10Shi-1) from the MHLW; HLSRG-H14nano001&genom005; the Promotion of Fundamental Studies in Health Science of the Organization for Pharmaceutical Safety and Research of Japan.

Manuscript received December 30, 2001; revised manuscript received July 2, 2002, accepted November 5, 2002.

Abbreviations and Acronyms

ANOVA	= analysis of variance
cDNA	= complementary deoxyribonucleic acid
DNA	= deoxyribonucleic acid
FGF4	= fibroblast growth factor 4
GHG	= gelatin hydrogel
lacZ	= beta-galactosidase
NIH	= National Institute of Health
PBS	= phosphate-buffered saline
pI	= isoelectric point
RNA	= ribonucleic acid
RT-nested PCR	= reverse transcription-nested polymerase chain reaction

mice (male ddY mice, six to seven weeks old, Shizuoka Animal Center, Shizuoka, Japan) were also used.

Preparation of GHG-DNA complex. DNA encoding FGF4, beta-galactosidase (lacZ) with the cytomegalovirus enhancer-chicken β-actin hybrid promoter comprising a cytomegalovirus enhancer, and chicken beta-actin promoter were constructed (12); GHG was prepared from bovine bone (6). The GHG used in this study was characterized by a spheroid shape with a diameter of approximately 200 μm, water content of 95%, and an isoelectric point (pI) of 11 after swelling in water, without special statement.

The efficiency of incorporation of DNA into positively and negatively charged GHG was evaluated. Dried GHG (4 mg, pI 11 or 5) was added to lacZ DNA solution (500 μg/100 μl in phosphate-buffered saline [PBS], pH 7.4), mixed with a vortex mixer for 5 s, and allowed to stand at 37°C; the solution immediately settled. The absorbance (260 nm) of the supernatant was measured. In a sham control experiment, GHG was added to pure PBS solution. Positively charged GHG (pI 11) was immediately impregnated with naked DNA, and was stable at pH 7.4 for at least 120 h, whereas the negatively charged one (pI 5) was not.

Experimental protocols. PROTOCOL 1: DNA DEGRADATION AND THE IMPROVEMENT OF TRANSFECTION EFFICIENCY BY GHG. To examine the temporal extension of gene degradation by GHG, the decay sequence of ^{125}I-labeled DNA impregnated into unlabeled GHG, ^{125}I-labeled GHG, and ^{125}I-labeled DNA solution was compared (63 mice). Plasmid DNA and GHG were radioiodinated with ^{125}I, with TlCl3 and Bolton and Hunter reagent (Amersham Pharmacia Biotech Ltd., Buckinghamshire, United Kingdom) (13), respectively. To impregnate GHG with DNA, dried GHG (2 mg) was added to 100 μl of naked lacZ solution (50 μg/100 μl in PBS), mixed for 5 s, and allowed to stand at 37°C for 2 h. Each complex was injected into the hindlimb muscle. On days 1, 3, 5, 7, 14, 21, or 28, the muscle was collected, and radioactivity was measured with a gamma counter (ARC-301B, Aloka Co., Ltd., Tokyo, Japan) in three mice each.

The following experiment was performed in 16 rabbits to assess spatial potentiation of gene expression by GHG. Intramuscular gene transfer was performed 10 days after modeling hindlimb ischemia. The DNA solution (FGF4-gene or lacZ 500 μg/100 μl PBS) mixed with GHG (4 mg; GHG-FGF4 complex, n = 2; GHG-lacZ complex, n = 2) and the original FGF4-gene solution (naked FGF4-gene, n = 2) were diluted with 0.4 ml saline and slowly injected through a 23-gauge needle at a single point in the adductor muscle marked with a 4-0 nylon suture. Tissue samples from the transfected left adductor muscle (the injection site and the adjacent region 10 mm apart from the injection site), the right adductor muscle, stomach, liver, spleen, testes, kidneys, heart, lungs, and brain were retrieved and immediately frozen in liquid nitrogen on day 17; FGF4-gene expression was evaluated by reverse transcription-nested polymerase chain reaction (RT-nested PCR). In the remaining 10 rabbits, gene expression was evaluated with lacZ gene; GHG-lacZ complex (n = 5) and naked lacZ solution (n = 5) were injected at a single point in the adductor muscle in the same way as the GHG-FGF4 injection on day 10. On day 17, a muscle sample at the injection site was dissected out, and expression of lacZ was determined by X-Gal histostaining (14).

PROTOCOL 2: SALVAGE OF HINDLIMB ISCHEMIA WITH GHG-PLASMID COMPLEX ENCODING FGF4. The angiogenic effect of three sets of GHG-DNA complexes were compared in 39 rabbits with hindlimb ischemia: 1) GHG impregnated with lacZ plasmid (GHG-lacZ: control); 2) naked FGF4-plasmid (naked FGF4-gene); and 3) GHG impregnated with FGF4 plasmid (GHG-FGF4). The amount of plasmid was 500 μg (1.0 ml) and that of GHG was 4 mg. On day 10 of ischemia, the gene complex was injected at five points 20 mm apart in the adductor muscle with a 23-gauge needle.

In 18 rabbits, on days 10 and 38 of ischemia, calf systolic blood pressure was measured by the Doppler flow signal from the posterior tibial artery (ES-100V2, Hayashi Denki Co., Kawasaki, Japan) with a 25-mm wide cuff. The calf blood pressure ratio of each rabbit was defined as the ratio of the systolic pressure of the ischemic limb to that of the normal limb. Regional blood flow was measured by the microsphere method (15) at baseline on days 0 and 38. On day 38, adenosine (100 μg/kg/min) was administered 30 min after baseline flow measurement (vasodilatory condition). A 4F catheter was introduced into the ascending aorta via the common carotid artery for microsphere injection and adenosine administration. Microspheres (15-μm diameter, 3 × 106) labeled with one of four sets of stable heavy elements (In, I, Ba, or Ce, Sekisui Plastic, Osaka, Japan) (15) were suspended in 0.05% sodium dodecyl sulfate at a concentration of 5 × 106/ml and injected into the ascending aorta. After killing the animals, the adductor, semimembranous, and gastrocnemius muscles were dissected out and weighed. The X-ray fluorescence of the labeled microspheres was measured in 4 to 8 g of the dissected muscles to calculate the regional blood flow (15) and expressed as the ratio of flow in the ischemic limb to flow in the normal limb.

JACC Vol. 41, No. 6, 2003
March 19, 2003:1056–62

Table 1. Morphologic Evaluation of Gene Therapy

Muscle Necrosis (Area)	GHG-lacZ	Naked FGF4	GHG-FGF4*†
Grade 0 (0 cm^2)	0	0	0
Grade 1 (<1 cm^2)	0	0	50% (3/6)
Grade 2 (<3 cm^2)	17% (1/6)	33% (2/6)	50% (3/6)
Grade 3 (<5 cm^2)	0	67% (4/6)	0
Grade 4 (<10 cm^2)	50% (3/6)	0	0
Grade 5 (>10 cm^2)	33% (2/6)	0	0
Muscle weight ratio (%)	48 ± 67 (6)	62 ± 14 (6)	79 ± 11* (6)

Morphologic indexes in 18 gene-transferred rabbits on day 38. The ischemic limb was macroscopically evaluated by using graded morphological scales for muscle necrosis area (the adductor, semimembranous, medial large, and gastrocnemius muscles) (grade 0 to 5); GHG-FGF4 group had significantly less muscle necrosis compared with naked FGF4 and GHG-lacZ groups. Muscle weight ratio was significantly different between GHG-FGF4 and GHG-lacZ groups. $p < 0.05$ vs. *GHG-lacZ, †naked FGF4 (Kruskal-Wallis test, analysis of variance).

FGF4 = fibroblast growth factor 4; GHG = gelatin hydrogel; lacZ = β-galactosidase.

Sufficient mixing of microspheres injected into the aorta (not into the left atrium) was confirmed by a preliminary study in which two different sets of microspheres were simultaneously injected into the aorta. The liner regression analysis on the two different sets of flows yielded an almost identical regression line ($y = 1.011x - 0.003$, $r = 0.98$, $Sy \cdot x = 0.032$). The remaining muscle tissue was used for histological analysis. An investigator blinded to the treatment macroscopically evaluated the ischemic limb on graded morphological scales for area of muscle necrosis (the adductor, semimembranous, medial large, and gastrocnemius muscles; grade 0 to 5; Table 1).

Synchrotron radiation microangiography characterized by high-resolution and high-sensitivity (16) was performed in 21 rabbits as previously described (15,17,18). The system is capable of separating adjacent lead lines only 20 μm apart on the resolution bar chart with 640× higher sensitivity than charge-coupled device camera system. This system allows detection and functional analysis of small vessels with a diameter of 200 to 500 μm in situ (15,17,18). Contrast material containing 37% nonionic iodine (Iopamidol, Nihon Schering Co., Tokyo, Japan) was injected via a 4F catheter placed immediately above the aortic bifurcation under baseline condition and during adenosine administration (100 μg/kg/min) (vasodilatory condition) via the same catheter. Vessel density in the midzone collateral was evaluated as an angiographic score (11,15,18).

Plasmid. Complementary deoxyribonucleic acid (cDNA) of human hst1/FGF4 (19), or bacterial β-galactosidase was inserted into the expression vector pRC/CMV (Invitrogen Corp., Carlsbad, California) and designated as pRC/CMV-HST1-10 (human stomach tumor) and pRC/CMV-lacZ, respectively. Preparation and purification of the plasmid from cultures of pRC/CMV-HST1-10-, or pRC/CMV-lacZ-transformed *Escherichia coli* were performed by centrifugation to equilibrium in cesium chloride-ethidium bromide gradients.

RT-nested PCR. Ribonucleic acid (RNA) was extracted from tissues with ISOGEN (Nippon Gene, Tokyo, Japan). The extracted RNA was treated with DNase twice to eliminate DNA contamination. In each set of experiments, 0.5 μg of total RNA was denatured at 70°C for 5 min, and reverse transcription was carried out at 37°C for 60 min; RT-nested PCR was carried out in a thermal cycler (GeneAmp PCR System 9600, Perkin Elmer, Wellesley, Massachusetts) with primers designed to selectively amplify the FGF4 cDNA. The external primers EcoHST1f3 (forward primer: GGA ATT CAC TGA CCG CCT GAC CGA CGC ACG GCC CTC G) and SalHST1r2 (reverse primer: GCG TCG ACC CCG AGG CTG AGG CAA GGG TCC TCT) were used for the first round (generating a 704-base pair [bp] fragment). The second round of the amplification (nested PCR) was performed with two internal primers HST1LGC1 (forward primer: AGC TCT CGC CCG TGG AGC GG) and HST1AA-r (reverse primer: CTC TGG AGG GTC ACA GCC TG) (generating a 282-bp fragment). The PCR reactions were performed as follows. The thermal cycle conditions for the first round were 30 cycles (95°C for 1 min, 59°C for 1 min, 72°C for 1 min), and for the second round were 25 cycles (94°C for 1 min, 72°C for 2 min), followed by incubation at 72°C for 10 min, respectively. Amplification products were detected after electrophoresis on 3.5% agarose gels by staining with ethidium bromide. A primer set of beta-actin (generating a 506-bp fragment) was used as a positive control for RT-PCR analysis.

Statistical analysis. Data are presented as mean values ± SD. Differences were assessed by using the paired *t* test, Kruskal-Wallis test, or analysis of variance (ANOVA) for factorial or repeated measures with the Scheffé F test when applicable. A value of $p < 0.05$ was considered statistically significant.

RESULTS

Protocol 1: DNA degradation and the improvement of transfection efficiency by GHG. The radioactivity of radiolabeled DNA impregnated into GHG in the limb muscle remained above the detection limit for four weeks (solid line in Fig. 1). The radiolabeled DNA impregnated into GHG had decay sequences almost identical to those of the radiolabeled GHG (dotted line in Fig. 1). By contrast, the radioactivity of naked DNA (dashed line in Fig. 1) decreased to <10% of the baseline within a day.

Gelatin hydrogel improved transfection efficiency in vivo; RT nested-PCR analyses revealed FGF4 expression at all injection sites in the left adductor muscle in the FGF4-gene-treated animals ($n = 4$), as shown in lanes 1 (naked FGF4-gene) and 4 (GHG-FGF4) in Figure 2; FGF4 expression was also detected in the adjacent region 10 mm apart from the injection site in the left adductor muscle in the GHG-FGF4-treated animals (lane 5), but not in the naked FGF4-gene-treated animals (lane 2). No expression was detected in any animal at remote sites, such as the right adductor muscle (lanes 3 and 6), stomach, liver, spleen,

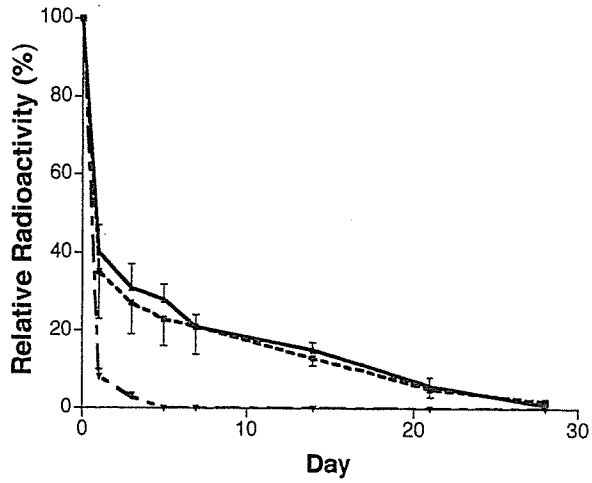

Figure 1. Decay sequences of radiolabeled deoxyribonucleic acid (DNA), gelatin hydrogel (GHG), and DNA combined with GHG in the hindlimb muscles of mice. Unlabeled GHG impregnated with ^{125}I-labeled DNA **(solid line)**, ^{125}I-labeled GHG **(dashed line)**, and ^{125}I-labeled DNA solution **(dotted line)** were injected into the hindlimb muscles.

testes, kidneys, heart, lungs, or brain (data not shown); lacZ-treated animals showed no FGF4 expression at any sites (lanes 7 and 8). Beta-actin expression was detected in all samples (lower panel), but neither beta-actin nor FGF4 expression was detected in any control samples that were not treated with reverse transcriptase; lacZ expression of naked DNA (500 μg) was localized to the injection site (Fig. 3A), whereas GHG-DNA complex (DNA amount 500 μg) showed a spatially expanded expression on day 17 (Fig. 3B). The degree of gene expression in myocytes was also augmented by GHG.

Protocol 2: salvage of hindlimb ischemia with GHG-plasmid complex encoding FGF4. Functional evaluation of ischemic hindlimbs showed amelioration of the ischemia

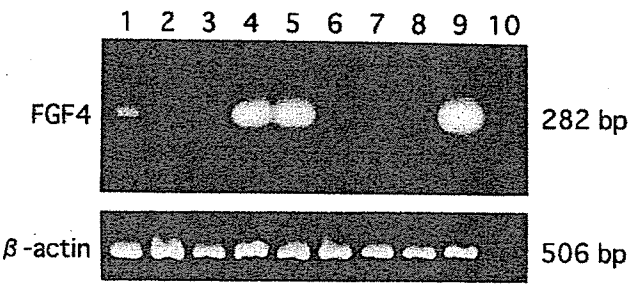

Figure 2. Representative transgene expression demonstrated by reverse-transcription nested polymerase chain reaction (RT-nested PCR). The left adductor muscle of the rabbits was injected with naked fibroblast growth factor 4 (FGF4) gene **(lanes 1 to 3)**, gelatin hydrogel (GHG)-FGF4 **(lanes 4 to 6)**, or GHG-lacZ **(lanes 7 and 8)**. Each sample was obtained from the injection site **(lanes 1, 4, and 7)** and the adjacent region 10 mm apart from the injection site **(lanes 2, 5 and 8)** in the left adductor muscle, and from the contralateral adductor muscle **(lanes 3 and 6)**. The RT-nested PCR products from ribonucleic acid of each sample were analyzed on agarose gel; FGF4 expressed Cc1/16 cells as a positive control **(lane 9)** and no deoxyribonucleic acid (DNA) template as a negative control **(lane 10)**. A housekeeping beta-actin gene was amplified as a complementary DNA loading control.

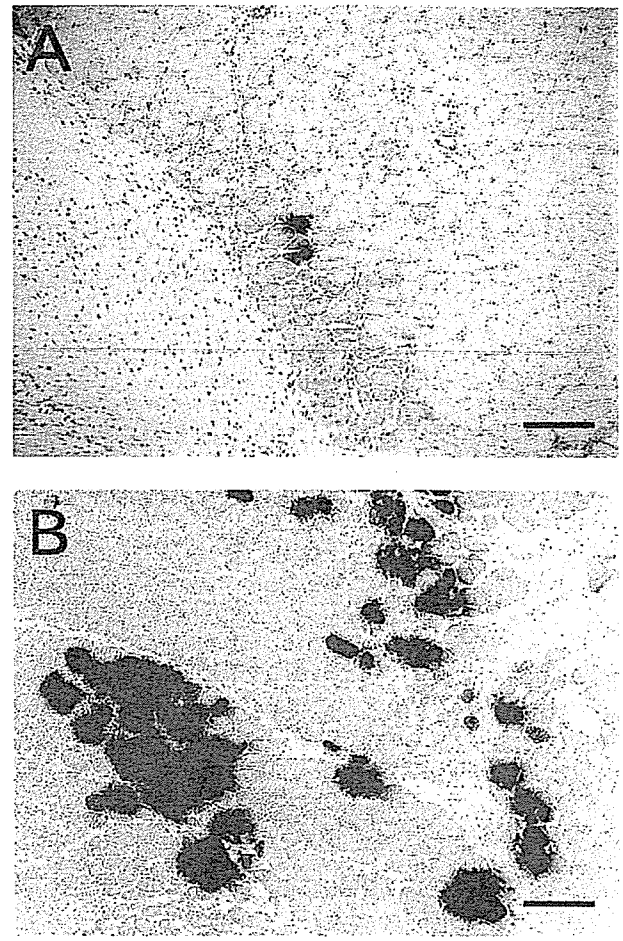

Figure 3. Representative gene expression of lacZ in the ischemic adductor muscle in rabbits on day 17. Naked deoxyribonucleic acid (DNA) **(A)** or gelatin hydrogel-DNA complex **(B)** was injected into the adductor muscle 10 days after the ischemic insult. X-Gal stain; original magnification ×20; **bar** = 200 μm.

by the FGF4-gene and potentiation of the amelioration when GHG was used as a delivery device. The augmentation of regional blood flow with GHG was more evident under vasodilatory conditions than at the baseline.

Regional blood flow analysis and angiographic analysis further confirmed the background mechanism for amelioration of hindlimb ischemia by GHG-FGF4 (Table 2). On day 38, blood flow during adenosine administration (vasodilatory condition) in the GHG-FGF4 group (105 ± 13% in terms of ischemic/normal flow ratio) was significantly higher than in either the naked FGF4-gene group (68 ± 18%, $p < 0.05$) or the GHG-lacZ group (50 ± 12%, $p < 0.05$, ANOVA). The differences between the naked FGF4-gene and GHG-lacZ groups were not significant (ANOVA). The adenosine-dependent flow-augmentation (responsiveness to vasodilatory stimulation; comparison between adenosine and baseline values on day 38) was noted only in the GHG-FGF4 group (from 79 ± 16% to 105 ± 13%, $p < 0.05$, ANOVA), and not in the other two groups. A similar tendency was noted in flow under baseline conditions on day 38 in all three groups; however, the

JACC Vol. 41, No. 6, 2003
March 19, 2003:1056–62

Table 2. Functional Evaluation of Gene Therapy

	GHG-lacZ	Naked FGF4	GHG-FGF4
Blood flow ratio (%) (ischemic/normal)			
Day 0 (BL)	33 ± 8 (6)	36 ± 11 (6)	37 ± 10 (6)
Day 38 (BL)	47 ± 12‡ (6)	58 ± 16‡ (6)	79 ± 16*‡ (6)
Day 38 (Ad)	50 ± 12‡ (6)	68 ± 18‡ (6)	105 ± 13*†‡§ (6)
Angiographic score			
Day 38 (BL)	0.37 ± 0.12 (7)	0.39 ± 0.13 (7)	0.42 ± 0.11 (7)
Day 38 (Ad)	0.36 ± 0.10 (7)	0.41 ± 0.13 (7)	0.56 ± 0.15*†§ (7)
Blood pressure (%) (ischemic/normal)			
Day 10	31 ± 8 (6)	33 ± 5 (6)	26 ± 7 (6)
Day 38	56 ± 4 (6)	63 ± 6 (6)	70 ± 11* (6)

Angiographic score was calculated on the synchrotron radiation microangiogram. $p < 0.05$ vs. *GHG-lacZ, †naked FGF4, ‡day 0 (BL), and §day 38 (BL) (analysis of variance).

Ad = during adenosine administration; BL = under baseline condition; FGF4 = fibroblast growth factor 4; GHG = gelatin hydrogel; lacZ = β-galactosidase.

differences in baseline flow among the three groups were less marked than during adenosine administration.

Synchrotron radiation microangiography revealed microvessel responsiveness to the vasodilatory stimulation in the GHG-FGF4-treated rabbits (Figs. 4C and 4D), whereas vascular density was somewhat decreased by adenosine treatment in some of the GHG-lacZ-treated rabbits (Figs. 4A and 4B). Angiographic score analysis yielded quantitative evidence (Table 2). The angiographic score during adenosine administration (vasodilatory condition) was significantly higher in the GHG-FGF4 group (0.56 ± 0.15) than in either the naked FGF4-gene group (0.41 ± 0.13, $p < 0.05$) or the GHG-lacZ group (0.36 ± 0.10, $p < 0.05$, ANOVA). By contrast, under baseline conditions, the angiographic scores of the three groups were not significantly different.

On day 38, the GHG-FGF4 group had the highest calf-blood pressure ratio (70 ± 11%), and it was lower in the naked FGF4-gene group (63 ± 6%), and even lower in the GHG-lacZ group (56 ± 4%, $p < 0.05$ vs. the GHG-lacZ group, ANOVA, Table 2). On day 10 (the time of gene transfer), the degrees of decrease in the three groups were not significantly different (26% to 33% in the mean).

Tissue damage was least in the GHG-FGF4-treated rabbits (Table 1). Limb muscle necrosis was <3 cm^2 and grade 1 or 2 in all of the animals in the GHG-FGF4 group, and significantly less than in the other two groups ($p < 0.05$, Kruskal-Wallis test). A similar difference was noted in the degrees of toe necrosis (data not shown). The muscle weight ratio (ischemic/normal) on day 38 was highest in the GHG-FGF4 group (79 ± 11%), lower in the naked FGF4-gene group (62 ± 14%), and even lower in the GHG-lacZ group (48 ± 67%), and the difference between the GHG-FGF4 group and GHG-lacZ group was significant ($p < 0.05$, ANOVA). The muscle weight ratio values (a morphological index) positively correlated with vascular responsiveness to adenosine (adenosine/baseline blood flow ratio [%]; a functional index) ($r = 0.50$, $n = 18$, $Sy \cdot x = 0.15$, $Sy \cdot x/y = 0.23$, $p = 0.045$). Thus, the blood flow, microangiographic, and morphologic analyses demonstrated a greater ameliorative effect of the GHG-FGF4 complex compared with the naked FGF4-gene (Tables 1 and 2).

Minimal inflammatory infiltrates, such as neutrophil and lymphoplasmacytic cell infiltrates, were noted at the injection site, but histological analysis showed that the infiltrates were localized. There was no evidence of fibrous proliferation or tumor formation in the transfected muscles or in other organs (right adductor muscle, stomach, liver, spleen, testes, kidneys, heart, lungs, and brain) in any of the groups.

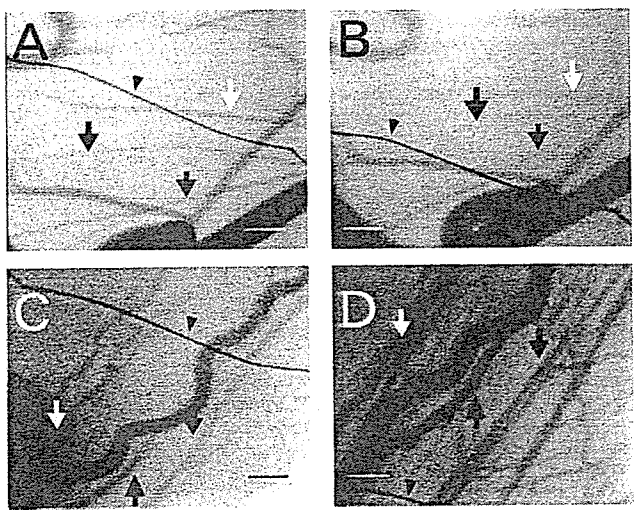

Figure 4. Representative synchrotron radiation microangiograms of the hindlimb ischemia in the rabbits. Synchrotron radiation microangiograms were taken under baseline conditions **(A and C)** and after repeated adenosine administration **(B and D)** on day 38. **(A and B)** Gelatin hydrogel (GHG)-lacZ-treated rabbit; **(C and D)** GHG-fibroblast growth factor 4-treated rabbit. **Arrows** indicate the same point in the vessels. **Arrowheads** reference copper wires with a diameter of 130 μm; **bar** = 1 mm.

DISCUSSION

We demonstrated that GHG potentiated the angiogenic effect of the FGF4-gene (protocol 2) by prolonging DNA degradation and improving transfection efficiency (protocol 1). Thus, GHG might facilitate the gene therapy of intractable circulatory disorders with genes for angiogenic growth factors.

Gelatin hydrogel augmented the effect of the FGF4-gene

therapy by improving gene biodegradation and transfection efficiency. We demonstrated that GHG rapidly absorbed plasmid DNA and did not release it in vitro (see Methods section). In the radioiodine experiment, the radioactivity of naked DNA was reduced to less than 10% of the baseline within a day, whereas the radioactivity of DNA impregnated into GHG remained for four weeks (Fig. 1). In the experiment using the rabbit hindlimb ischemia model, the PCR analysis suggested that GHG expanded the gene transfer spatially (lanes 2 and 5 in Fig. 2). The maker gene experiment (protocol 1) confirmed that the use of GHG augmented both the number of transfected myocytes and the degree of gene expression in these cells, and also supported the spatially expanded gene expression (Fig. 3). The superiority of the therapeutic effects of the GHG-FGF4-gene complex on hindlimb ischemia compared with naked FGF4-gene treatment was confirmed in the rabbit experiments in protocol 2 (Fig. 4, Tables 1 and 2); GHG-FGF4-treated rabbits were characterized by less severe tissue damage in the ischemic limb (Table 2) and more marked vascular responsiveness to adenosine than either the naked FGF4-treated or GHG-lacZ-treated rabbits (Fig. 4, Table 2, Protocol 2 in the Results section). Under the baseline conditions, blood flow in normal muscle tissue is set at a relatively low level in preparation for an abrupt increase in flow demand (approximately 5× and 30× in the heart and in the skeletal muscle, respectively) during exercise, etc. (responsiveness to the vasodilatory stimulation). In other words, normal muscle tissue has a sufficient flow reserve (20,21), and, thus, the presence or absence of vascular responsiveness to adenosine administration can be used as an index of fundamental vascular function in angiogenic vascular segments. The demonstration of a positive correlation between flow responsiveness to adenosine and the muscle weight ratio further supports our hypothesis. Baseline flow may reflect the total number of angiogenic vessels, if it does not respond to vasodilatory stimulation. However, if the vasodilatory mechanism is present, baseline flow alone does not necessarily reflect the quality and/or quantity of angiogenic vascular segments. The amelioration of the ischemic tissue in the GHG-FGF4 group may be related to an adequate flow reserve (20,21) of so-called "well-tempered angiogenic vessels" (22).

Consequently, GHG offers several advantages as a new gene delivery system: 1) it has a positively charged structure, so it holds negatively charged nucleic acids, proteins, and drugs within its structure; 2) GHG is biodegradable and implantable; the biodegradable nature is from the gelatin itself but not from the hydrogel state. The substance bound to the GHG is gradually released as the gelatin degrades in situ. The degradation period can be adjusted to two to four weeks by varying the water content. Thus, the prolonged release of the DNA held in GHG was presumably responsible for the augmentation of gene therapy. The use of hydrogel-coated balloon-angioplasty-catheter has been reported (7). However, this gel is much different from our hydrogel. The present GHG consists of amino acids and is biodegradable and implantable, whereas their hydrogel consists of carbohydrate and is not biodegradable nor implantable. 3) The isoelectric point and the shape of the GHG can be modified. Negatively charged GHG holds positively charged substances such as basic-FGF protein (6,23), and disk-shaped GHG has been found to be effective for reconstruction of bone defects (23); 4) GHG is less biohazardous than adenovirus vectors. Gelatin is already used in the clinical field, and its safety is established. Thus, the use of GHG with naked DNA improves its transfection efficiency without causing serious cytotoxicity or biohazards, which are inconvenient side effects of virus vectors (24). Therefore, the nonvirus vector GHG is useful for various gene therapies including the treatment of cardiovascular disorders.

Acknowledgments

The authors wish to thank Chiharu Tada, Akiko Hori, Sachie Ueno, and Takayuki Hasegawa for their technical work.

Reprint requests and correspondence: Dr. Hidezo Mori, Department of Cardiac Physiology, National Cardiovascular Center Research Institute, 5-7-1 Fujishirodai, Suita 565-8565, Japan. E-mail: hidemori@ri.ncvc.go.jp.

REFERENCES

1. Asahara T, Bauters C, Zheng LP, et al. Synergistic effect of vascular endothelial growth factor and basic fibroblast growth factor on angiogenesis in vivo. Circulation 1995;92:417–27.
2. Aoki M, Morishita R, Taniyama Y, et al. Angiogenesis induced by hepatocyte growth factor in non-infarcted myocardium and infarcted myocardium: up-regulation of essential transcription factor for angiogenesis. Gene Ther 2000;7:417–27.
3. Yang Y, Trinchieri G, Wilson JM. Recombinant IL-12 prevents formation of blocking IgA antibodies to recombinant adenovirus and allows repeated gene therapy to mouse lung. Nat Med 1995;1:890–3.
4. Zabner J, Ramsey BW, Meeker DP, et al. Repeat administration of an adenovirus vector encoding cystic fibrosis transmembrane conductance regulator to the nasal epithelium of patients with cystic fibrosis. J Clin Invest 1996;97:1504–11.
5. Takeshita S, Isshiki T, Sato T. Increased expression of direct gene transfer into skeletal muscles observed after acute ischemic injury in rats. Lab Invest 1996;74:1061–5.
6. Tabata Y, Hijikata S, Muniruzzaman M, Ikada Y. Neovascularization effect of biodegradable gelatin microspheres incorporating basic fibroblast growth factor. J Biomater Sci Polym Ed 1999;10:79–94.
7. Isner JM, Pieczek A, Schainfeld R, et al. Clinical evidence of angiogenesis after arterial gene transfer of phVEGF165 in patients with ischaemic limb. Lancet 1996;348:370–4.
8. Sakamoto H, Mori M, Taira M, et al. Transforming gene from human stomach cancers and a noncancerous portion of stomach mucosa. Proc Natl Acad Sci USA 1986;83:3997–4001.
9. Fuller PF, Peters G, Dickson C. Cell transformation by kFGF requires secretion but not glycosylation. J Cell Biol 1991;115:547–55.
10. Yoshida T, Ishimaru K, Sakamoto H, et al. Angiogenic activity of the recombinant hst-1 protein. Cancer Lett 1994;83:261–8.
11. Takeshita S, Zheng LP, Brogi E, et al. Therapeutic angiogenesis: a single intra-arterial bolus of vascular endothelial growth factor augments revascularization in a rabbit ischemic hind limb model. J Clin Invest 1994;93:662–70.
12. Miyazaki J, Takaki S, Araki K, et al. Expression vector system based on the chicken beta-actin promoter directs efficient production of interleukin-5. Gene 1989;79:269–77.

JACC Vol. 41, No. 6, 2003
March 19, 2003:1056–62

13. Bolton AE, Hunter WM. The labelling of proteins to high specific radioactivities by conjugation to a ^{125}I-containing acylating agent. Biochem J 1973;133:529–39.
14. Ueno H, Li JJ, Tomita H, et al. Quantitative analysis of repeat adenovirus-mediated gene transfer into injured canine femoral arteries. Arterioscler Thromb Vasc Biol 1995;15:2246–53.
15. Tanaka E, Hattan N, Ando K, et al. Amelioration of microvascular myocardial ischemia by gene transfer of vascular endothelial growth factor in rabbits. J Thorac Cardiovasc Surg 2000;120:720–8.
16. Tanioka K, Yamazaki J, Shidara K, et al. Avalanche-mode amorphous selenium photoconductive target for camera tube. Adv Electronics Electron Phys 1988;74:379–87.
17. Mori H, Hyodo K, Tanaka E, et al. Small-vessel radiography in situ with monochromatic synchrotron radiation. Radiology 1996;201:173–7.
18. Takeshita S, Isshiki T, Ochiai M, et al. Endothelium-dependent relaxation of collateral microvessels after intramuscular gene transfer of vascular endothelial growth factor in a rat model of hindlimb ischemia. Circulation 1998;98:1261–3.
19. Taira M, Yoshida T, Miyagawa K, Sakamoto H, Terada M, Sugimura T. cDNA sequence of human transforming gene hst and identification of the coding sequence required for transforming activity. Proc Natl Acad Sci USA 1987;84:2980–4.
20. Austin RJ, Aldea GS, Coggins DL, Flynn AE, Hoffman JI. Profound spatial heterogeneity of coronary reserve: discordance between patterns of resting and maximal myocardial blood flow. Circ Res 1990;67:319–31.
21. Coggins DL, Flynn AE, Austin RJ, et al. Nonuniform loss of regional flow reserve during myocardial ischemia in dogs. Circ Res 1990;67:253–64.
22. Blau H, Banfi A. The well-tempered vessel. Nat Med 2001;7:532–4.
23. Yamada K, Tabata Y, Yamamoto K, et al. Potential efficacy of basic fibroblast growth factor incorporated in biodegradable hydrogels for skull bone regeneration. J Neurosurg 1997;86:871–5.
24. Marshall E. Gene therapy death prompts review of adenovirus vector. Science 1999;286:2244–5.

Journal of Cardiovascular Pharmacology™
41 (Suppl. 1):S111–S114 © 2003 Lippincott Williams & Wilkins, London

Effects of Moderate Hypothermia on Norepinephrine Release Evoked by Ouabain, Tyramine and Cyanide

Hirotoshi Kitagawa, *Toji Yamazaki, *Tsuyoshi Akiyama, *Hidezo Mori and †Kenji Sunagawa

*Department of Anesthesia, Nagahama City Hospital, Nagahama, Japan; *Department of Cardiac Physiology and †Department of Cardiovascular Dynamics, National Cardiovascular Center, Research Institute, Suita, Japan*

Summary: Using the dialysis technique, we examined the effect of moderate hypothermia on the norepinephrine efflux evoked by ouabain, tyramine and cyanide in anesthetized cats. Dialysis probes were implanted in the left ventricular myocardium, and we measured the dialysate norepinephrine levels as an indicator of norepinephrine output at the cardiac sympathetic nerve endings. Through the dialysis probe, locally applied ouabain, tyramine and cyanide induced the norepinephrine efflux. The addition of desipramine (neuronal norepinephrine transport blocker, 100 μM) suppressed the norepinephrine efflux evoked by ouabain, tyramine and cyanide. This finding suggests that pharmacological agent-induced norepinephrine efflux was due to carrier-mediated outward norepinephrine transport. Moderate hypothermia (27.4 ± 0.2°C) caused suppression of the norepinephrine efflux evoked by ouabain, tyramine and cyanide. We conclude that moderate hypothermia suppresses the non-exocytotic norepinephrine release evoked by ouabain, tyramine and cyanide. **Key Words:** Desipramine—Dialysis technique—Heart—Norepinephrine—Sympathetic nerve.

Temperature is known to influence the kinetics of neurotransmitters at the nerve endings (1,2). *In vitro* studies have demonstrated that the processes of norepinephrine (NE) release, uptake and vesicle transport at sympathetic nerve endings are greatly suppressed under low-temperature conditions (1). However, these experiments were carried out at room temperature or profound low temperatures. It is uncertain whether these processes are also inhibited in clinically applied moderate hypothermia. We recently demonstrated that moderate hypothermia inhibits exocytotic NE release from cardiac sympathetic nerve endings, with this inhibition of NE release associated with impairment of vesicle NE transport but not with impairment of NE uptake (3).

In addition to inhibitory action of exocytotic NE release, moderate hypothermia modulates intraneurnal NE kinetics at the sympathetic nerve endings. Actually, moderate hypothermia affects axoplasmic NE concentrations (3). The impairment of vesicle NE transport elevated axoplasmic NE levels, indicating the possibility that moderate hypothermia augments non-exocytotic NE release. However, moderate hypothermia has been reported to exert greater suppression of non-exocytotic NE release than of exocytotic NE release (4). Thus, the evidence for the effect of moderate hypothermia on non-exocytotic NE release is controversial. Although non-exocytotic NE release plays an important role in such pathophysiological conditions as ischemia and anoxia (5,6), how moderate hypothermia modulates non-exocytotic NE release remains to be determined.

We tested the hypothesis that moderate hypothermia affects non-exocytotic NE release. We used several pharmacological agents considered to induce non-exocytotic NE release and examined whether moderate hypothermia modulates non-exocytotic NE release. In the present study, to test this hypothesis, we applied the microdialysis approach to the left ventricle in anesthetized cats (7). First, we investigated the contribution of membrane NE transporter to the NE efflux evoked by local administration of pharmacological agents. Second, we investigated

Address correspondence and requests for reprints to Hirotoshi Kitagawa, Department of Anesthesiology, Shiga University of Medical Science, Otsu 520-2192, Japan. Email: hirotosi@belle.shiga-med.ac.jp